Turbulence Characteristics in Tidal Flows Using LES and ALM to Model the Tidal Power Plant Deep Green

Sam T. Fredriksson[#1], Göran Broström[#2], Björn Bergqvist[*3], Johan Lennblad[*4], and Håkan Nilsson[#5]

[#1-2]*Department of Marine Sciences, University of Gothenburg, Gothenburg, Sweden*
[#5]*Department of Mechanics and Maritime Sciences, Chalmers University of Technology, Gothenburg, Sweden*

[1]sam.fredriksson@gu.se

[2]goran.brostrom@marine.gu.se

[5]hakan.nilsson@chalmers.se

[*3-4]*Minesto AB Gothenburg, Sweden*

[3]bjorn.bergqvist@minesto.com

[4]johan.lennblad@minesto.com

Abstract— **The turbulence in tidal flows affects the design and operation of tidal plants, e.g., through control system and dynamical loads. Present work is focused on a specific site west of Holy Island along the north west cost of Wales and a specific tidal power plant, Deep Green. Although, specific and applied, the work is generally applicable regarding findings and modelling techniques for other sites and designs.**

Large Eddy Simulations (LES) are used to study first the undisturbed tidal flow and then the flow with a power plant in operation. The undisturbed tidal flow simulations show that the turbulence characteristics differ between the acceleration and deceleration phase of the tidal cycle. The turbulence statistics are also used to estimate dynamical loads on the tidal plant with respect to, e.g., fatigue.

Secondly, a novel Actuator Line Method (ALM) tidal power plant model, that e.g., takes the arbitrary trajectories of the power plant wing into account, is used. It's used to study how the power plants affect the environment, available power downstream, and turbulence characteristics affecting other power plants in possible power plant arrays. It is shown that the width of the trajectory can be used as a measure to estimate the wake extent.

Keywords— **Tidal energy, Turbulence, Large Eddy Simulation (LES), Actuator Line Method (ALM).**

I. Introduction

Several new technologies are emerging for power extraction from tidal currents. They span from devices that operates at the surface or in mid-depth, to turbines mounted on the bottom [1]. The power plants will typically operate in regions with strong tidal currents which implies that robust equipment design becomes an important. Turbulence characteristics of tidal currents have been targeted in some studies [2-4] and how bottom mounted turbines operate in and affect a tidal flow have been studied in [5-7]. The turbulence intensity and length scale of the turbulent eddies have been focused in the main part of the studies, whereas other quantities such as structure functions, probability density functions, intermittency, coherent turbulence kinetic energy, anisotropy invariants, and a scalar measure of anisotropy to characterize the turbulence have been suggested as interesting features of the turbulence as well [8]. In this work, computational fluid dynamic modelling is used to describe and estimate the turbulence fields and their impact on the structure.

Both tidal current and wind power plants reduce the velocity and affect the turbulence characteristics downstream of the plants. Wind power plants and farms of wind power plants have a much longer industrial history and have therefore been more thoroughly studied [9-10] as compared to tidal current power plants. It has been shown for wind power plants that the persistence of the disturbance in the flow field (wake) is affected by the roughness of the ground; an increase of the roughness decreases the persistence and vice versa. It has further been seen that the mixing in the lower atmosphere is increased by land based wind farms [11-12] and that offshore wind farms force local vertical mixing [13]. The vertical mixing in shallow coastal water is constrained by the sea surface boundary which in turn probably increase the importance of horizontal mixing of the wake for tidal current compared to wind power plants. This difference would imply that planning and optimization of power plant arrays are even more important for tidal current than wind power plants. There are a few studies regarding optimization of energy capture of tidal power arrays [14-17]

A. Deep Green technology

The main component of this power plant is a tethered kite flying through water, where the wing is pushed forward by the moving water, as shown in Fig. 1. The motion is to some extend braked by a turbine, and then there is conventional technique to transform the braked power to useful electricity. In its current design, the length of the wing is 12 meters and the rated power of the generator is 500 kW.

The main components in the system model, used for control system and force analysis, is the kite, the tether and a control system to actuate rudder, elevator and pitch of the kite. The art in building useful models on a high system level is to simplify

as much as possible thus condensing it to the most critical sections.

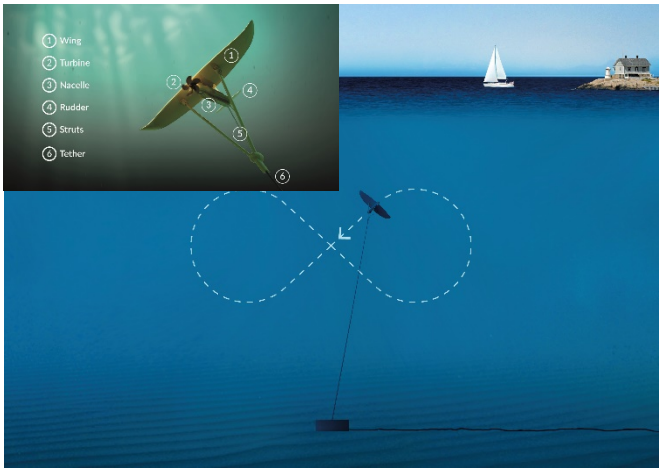

Fig. 1 Illustration of the Deep Green device where it forms a trajectory (lemniscate) approximately perpendicular to the tidal flow during operation.

Initially, it is therefore natural to consider the tidal flow as essentially a plug flow. In fact, the majority of questions asked to the system model can be responded in this way. It is, however, clear from tests and engineering judgement that the water turbulence has a definite impact on the kite. Also, the tidal current is not homogenous from sea floor to the surface, and knowledge about velocity variation with water depth is crucial for a well optimised kite.

Turbulence introduces stochastic variations of the flow velocity. It is characterised by flow vortex ranging in size from characteristic dimensions of the kite down to very small length scales. It is therefore reasonable to assume that turbulence impacts the kite path and actuator control and also high frequency oscillations, which are a potential threat to material fatigue.

II. Methods

Large Eddy Simulations (LES) is used to analyze the tidally oscillating turbulent boundary layer flow. The pseudo-spectral modelling technique is used for the undisturbed flow without the Deep Green whereas a finite volume method is used for the cases with Deep Green, see Fig. 2 and Table 1. The Deep Green is modeled using the Actuator Line Method (ALM) reformulated in order to be able to take the arbitrary pathway of the Deep Green into account [18-19]. In ALM the body forces are modeled as source terms using a blade-element approach. It is used since a resolved wing model would be too resource demanding taking into account the need of a sufficient large computational domain and long simulation time. The results from the pseudo-spectral model are used both for the control system and force analysis in Dymola and as initial conditions for the precursor LES, see Fig 3. The precursor LES is an intermediate step that uses the results from the tidal cycle LES as initial conditions and tidal forcing to give fully turbulent upstream boundary conditions to be used in the Deep Green LES using ALM. All LES models model the sub-grid scale stress tensor via the one-equation eddy-viscosity concept, using a transport equation for the sub-grid scale kinetic energy and a local length scale [18].

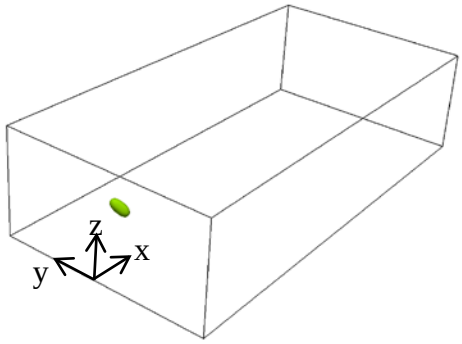

Fig. 2 Extent of the computational domain where the Deep Green (close to the upstream boundary) is indicated at the centre of its trajectory. Modified from [18].

TABLE I
Computational setup for LES

Description	Code	Domain[1]	Resolution[2]	Force[3]
Tidal cycle	NCAR-LES	16, 4, 1	2048, 512, 128	F_T
Precursor	OpenFOAM	4, 2, 1	512, 256, 128	F_T
Deep Green	OpenFOAM	4, 2, 1	512, 256, 128	F_{DG}

[1] Size relative to depth, $H = 80\ m$, in x, y, and z directions.
[2] In x, y, and z directions (equidistant).
[3] Tidal force, F_T, and Deep Green force, F_{DG}, respectively.

The control system, force, and lemniscate analyses are performed using the Dymola software. Dymola is a general purpose simulation tool for dynamic systems. It is structured in an object oriented way, which implies easy reuse of models and a straight forward way to combine different types of physics in one model. Models in Dymola are therefore in particular suitable to be combined into complete systems. The Deep Green Dymola model includes subsystems for the kite itself, the tether as an elastic component with many degrees of freedom, the control system as well as the tidal current environment of the kite. This model can be extended, depending on needs to also include the hydraulic systems to control the actuators and more details of the electrical system to convert mechanical turbine work to useful electric power. These analyses are both an input to the Deep Green LES as well as the tidal cycle and/or Deep Green LES subsequently give input to further simulations within Dymola.

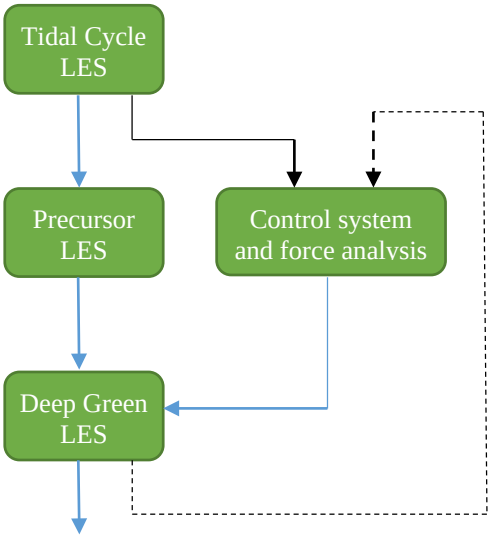

Fig. 3 Sketch of work flow. Blue arrows show the path when plug flow is used in the control system analysis to produce lemniscate input to Deep Green LES. Black solid line shows when tidal Cycle LES is used as input to control system and force analysis and dashed black line show how Deep Green LES can be used as input for control system analysis for tidal power array analysis.

The first Deep Green is to be deployed west of Holy Island along the north west coast of Wales and the model is setup to resemble this site condition. Here, the depth is approximately $80\ m$ and observations report frequent boulders with dimensions of roughly $2 \times 2 \times 2\ m^3$ at the bottom, which is modeled using a bottom roughness length. A full tidal cycle (12 h) sinusoidal body force is used to force the flow. Its amplitude is adjusted to give the maximum tidal peaks present at the site ($1.6, 2.0$, and $2.4\ ms^{-1}$ respectively). We assume that Coriolis force perpendicular to the main flow is balanced by a pressure gradient. Fig. 4 shows the volume mean flow in the tidal cycle LES during a number of tidal cycles for the case with a maximum tidal peak of $2.0\ ms^{-1}$.

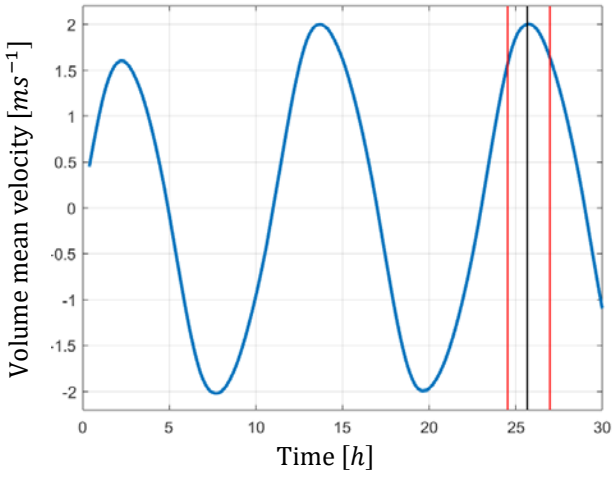

Fig. 4 Volume mean tidal flow. The instance for the third tidal peak (between 25 and 26 h) and where the volume mean flows of $1.6\ ms^{-1}$ are indicated with a black line and red lines, respectively. The instantaneous field at the time marked with the first red line (approx. 24.5 h) is used as initial conditions for the simulation with the Deep Green.

III. Results and Discussion

Here some preliminary results from the tidal cycle LES, Deep Green LES, and Dymola control system and force analysis are presented.

A. *Tidal cycle LES*

The main objective in this study regarding the tidal cycle LES is to give snapshots of the fully turbulent velocity fields as a function of time to be used in the control system and force analysis. It is, however, also of interest to study its turbulence characterises from a more statistical and fundamental point of view in order to increase the general knowledge of tidal current flow. The turbulence intensity $I = \sigma(q)/\overline{U}(z)$ is presented in Fig. 5 for the case with a maximum tidal peak of $2.0\ ms^{-1}$.

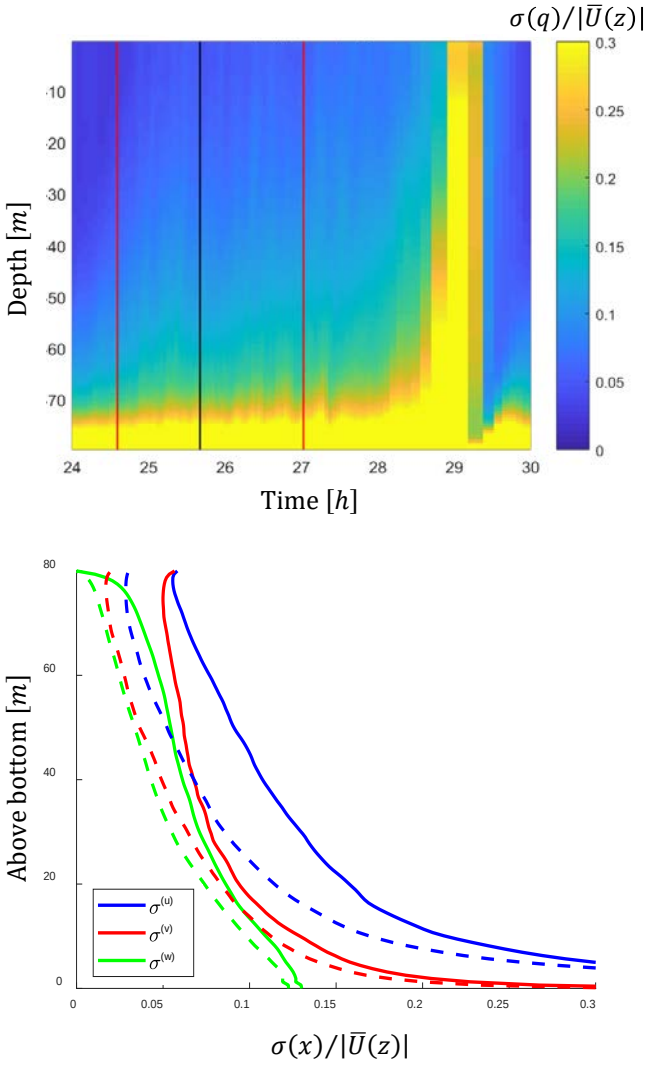

Fig. 5 Turbulence intensity. The instance for the third tidal peak (between 25 and 26 h) and where the volume mean flows of $1.6\ ms^{-1}$ are indicated with a black line and red lines, respectively. Dashed lines before and full line after the tidal peak, respectively.

Here $\sigma^2(q) = Var(q)$, $\bar{U}(z)$ is the horizontal mean velocity, Var is the variance, $q(u, v, w)$ is the velocity fluctuation in the coordinate directions x, y, and z. The black and red lines in Fig. 5. follow the Fig. 4. The figure zooms in around the third tidal peak (between 25 and 26 h) marked with a black line. The red lines mark the occasions where the volume mean flows is 1.6 ms^{-1}. It is seen that the turbulence intensity varies strongly with time and is asymmetric around the tidal peak with higher intensity in the deceleration as compared to the acceleration phase. It is further noticed that the intensity is anisotropic in different directions with the highest intensity in the stream wise direction and lowest in the vertical direction.

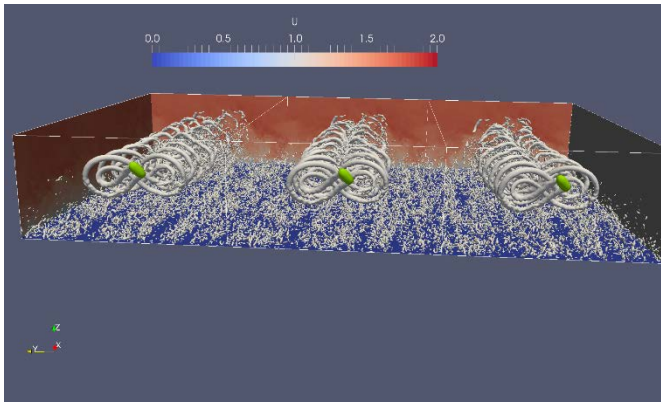

Fig. 6 Instantaneous velocity fields at the domain boundaries and isosurfaces of the second invariant of the velocity gradient tensor (which indicate vortices) in grey. The Deep Green position is visualized by a green isosurface of the force field. Here three computational domains (with cyclic boundaries in the x-direction) have been plotted beside each other in order to give a first impression of how possible power plant arrays would look like and how the power plants affect each other depending on the array configuration.

The stream wise velocity deficit downstream of the Deep Green is given in Fig. 7. It can be seen that there are a substantial influence in the velocity field at least $4D_y$ downstream of the lemniscate both horizontally and vertically.

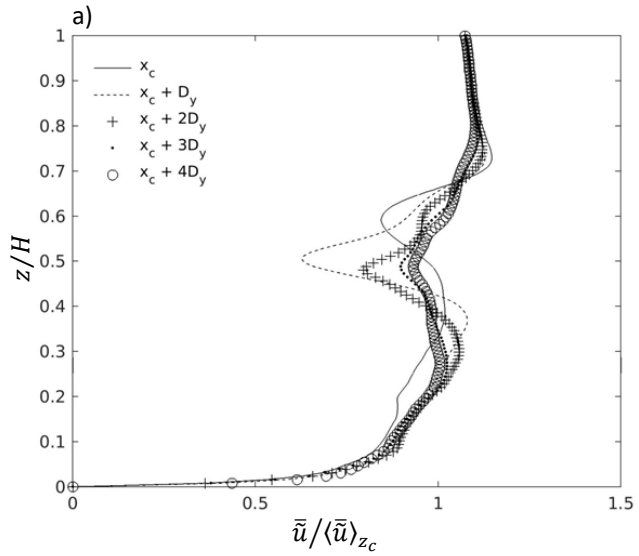

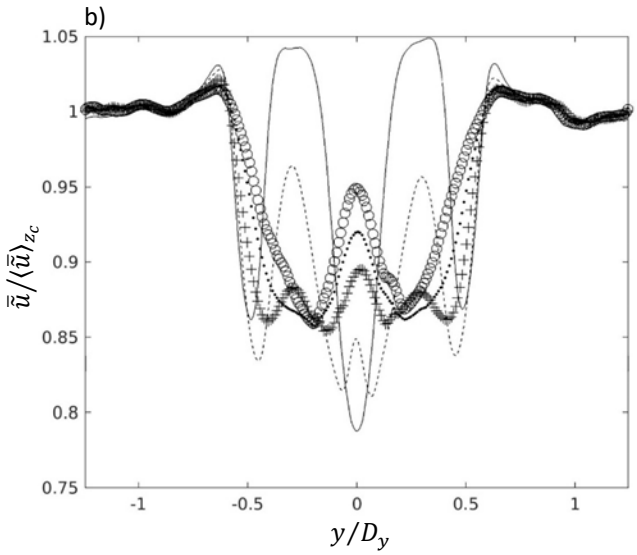

Fig. 7 Velocity deficit (streamwise). Comparison of mean flow velocities, at locations downstream of the Deep Green trajectory centre (x_c, y_c, z_c), show the downstream wake. a) Vertical profiles at the yz-planes, through $y = y_c$. b) Horizontal profiles at the yz-planes, through at $z = z_c$.

B. Control system and force analysis

The Fig. 8-11 show results from a control system and force simulation for the kite. In this simulation a plug flow is assumed for the first 200 s. After this period the flow is shifted to turbulent and including the velocity depth variation (mapping the results from tidal cycle LES). This mapped turbulence is computed beforehand neglecting the kite impact on the flow. Since these computations are demanding with respect to both time and data storage, the turbulent period used here lasts for about 250 s. When Dymola eventually arrives at the last time step the turbulent time series repeats itself.

Fig. 8 shows the kite flying in production mode following its lemniscate very well. There is really no sign of the path being wiggly when passing into the turbulent flow.

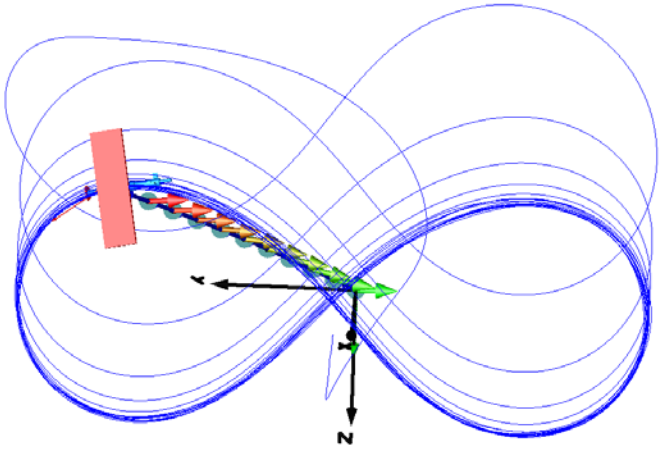

Fig. 8 The kite path during the complete flight. It follows the lemniscate well, and there is no distinct point visible when the kite enters the turbulent region.

Fig. 9 shows the kite velocity, tidal flow velocity and the rudder angle. It is clearly seen in the tidal flow velocity that the kite enters the turbulent region at 200 s, which in turn also makes a notable impact on kite velocity. The rudder angle signal is, however, not much impacted. Fig. 10. shows the angle of attack at the middle sections and at two points half way to the wing tip on each sides respectively. It can be seen that the turbulence much spikier with sharper gradient than for a plug flow. Finally, Fig. 11 shows the tether force. It is seen to be impacted by the turbulence, and therefore it can be concluded that turbulence will have an impact on fatigue.

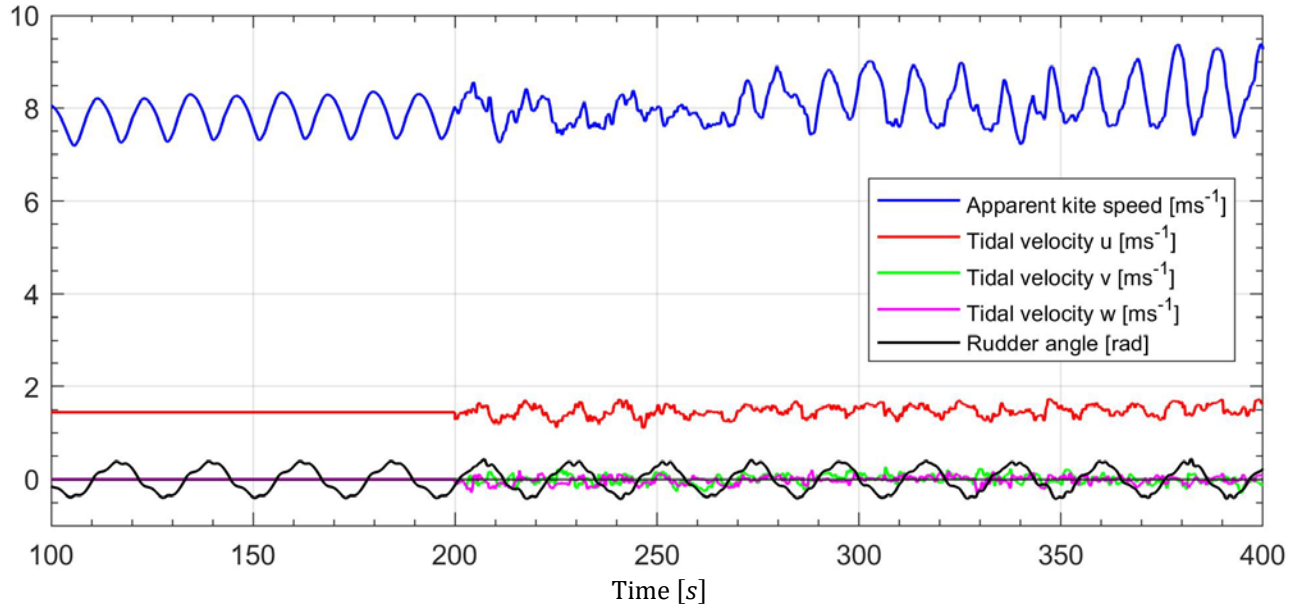

Fig. 9 The Kite velocity (blue), rudder angle (black) and the three tidal velocity components. The turbulent region starts after 200 s.

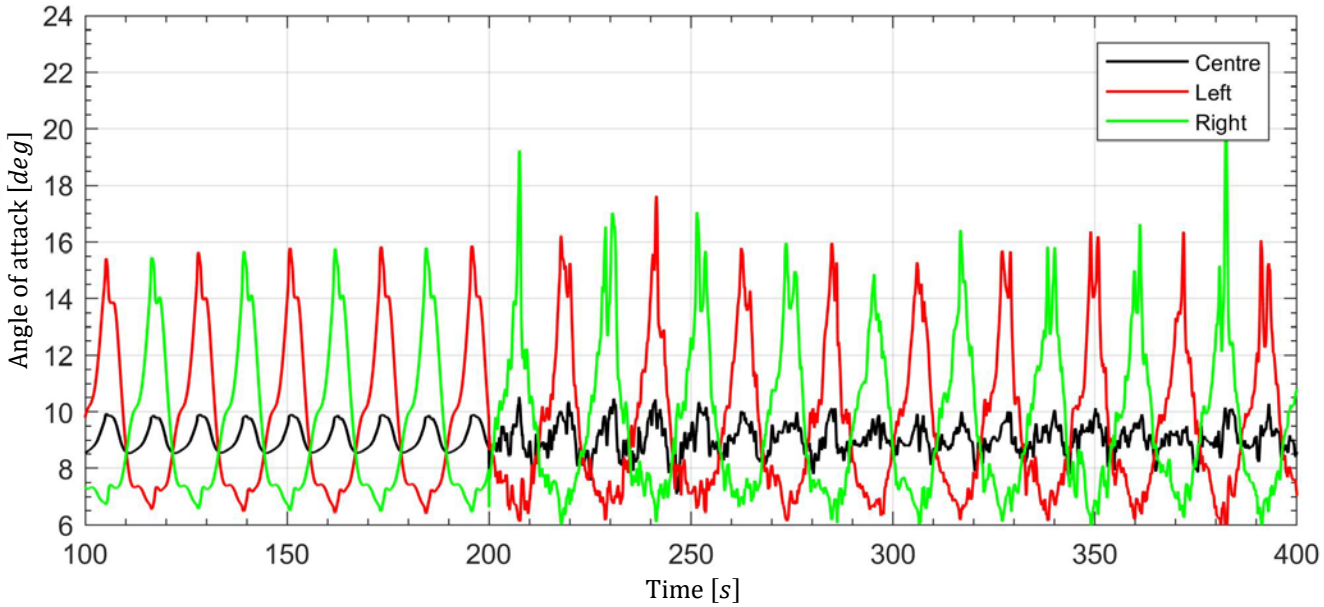

Fig. 10 The angle of attack at wing centre (blue) and half way to wing tip (red and green). The turbulent region starts after 200 s.

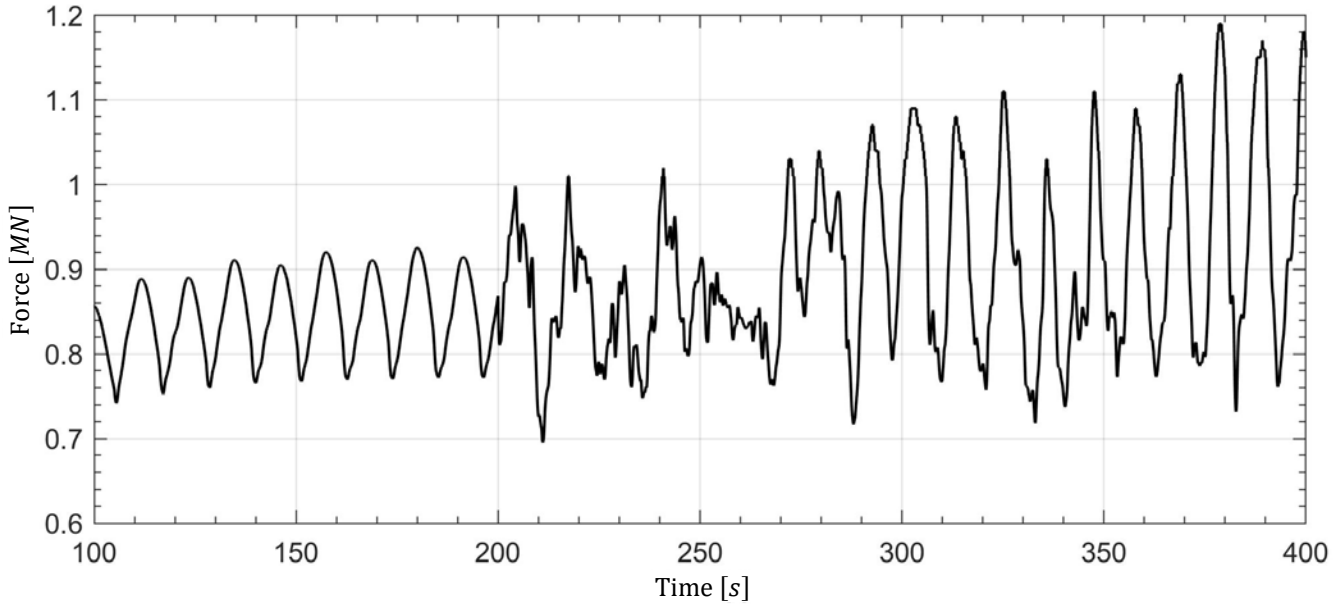

Fig. 11 The tether force. The turbulent region starts after 200 s.

IV. Conclusions

The overall aim for this work is to find the turbulent characteristics of tidal flow, undisturbed and with power plants, and how it in turn affects power plants and the environment. This is achieved by creating a work process using three computational models. The trajectory and control system of, and the forces at, the power plant is studied in Dymola. The turbulence is studied using large eddy simulations in undisturbed tidal-cycle simulation using a pseudo-spectral approach in NCAR-LES and in model using an actuator line method to model the power plant in a finite-volume approach in OpenFOAM.

The results show that the turbulence intensity is time dependent and differs comparing the accelerating and deceleration phase for the same volume mean flow. It is also seen to be anisotropic with the highest intensity in the flow direction.

The wake extension can be characterized with the horizontal width of the lemniscate. The model will be able to study eventual tidal power arrays.

The undisturbed turbulence does not disturb the lemniscate of the deep green but it influences, e.g., the rudder angle signal and the kite velocity. It can also be seen that the tether force is affected both regarding an increase in the amplitude and with a spikier signal which might have fatigue implications

Acknowledgment

This project is financed by the Swedish Energy Agency. The simulations for undisturbed tidal flow were performed on resources provided by the Swedish National Infrastructure for Computing (SNIC) at C3SE.

References

[1] D. Magagna, R. Monfardini, and A. Uihlein, *JRC Ocean Energy Status Report 2016 Edition.* 2016.

[2] M. Lewis, et al., *Characteristics of the velocity profile at tidal-stream energy sites.* Renewable Energy, 2017. 114: p. 258-272.

[3] A. Mason-Jones, et al., *Non-dimensional scaling of tidal stream turbines.* Energy, 2012. 44(1): p. 820-829.

[4] I.A. Milne, et al., *Characteristics of the turbulence in the flow at a tidal stream power site.* Philosophical Transactions of the Royal Society a-Mathematical Physical and Engineering Sciences, 2013. 371(1985).

[5] T. Blackmore, L.E. Myers, and A.S. Bahaj, *Effects of turbulence on tidal turbines: Implications to performance, blade loads, and condition monitoring.* International Journal of Marine Energy, 2016. 14: p. 1-26.

[6]. U. Ahmed, et al., *Fluctuating loads on a tidal turbine due to velocity shear and turbulence: Comparison of CFD with field data.* Renewable Energy, 2017. 112: p. 235-246.

[7] A. Mason-Jones, et al., *Influence of a velocity profile & support structure on tidal stream turbine performance.* Renewable Energy, 2013. 52: p. 23-30.

[8] K. McCaffrey, et al., *Characterization of turbulence anisotropy, coherence, and intermittency at a prospective tidal energy site: Observational data analysis.* Renewable Energy, 2015. 76: p. 441-453.

[9] R.J. Barthelmie and L.E. Jensen, *Evaluation of wind farm efficiency and wind turbine wakes at the Nysted offshore wind farm.* Wind Energy, 2010. **13**(6): p. 573-586.

[10] R.J. Barthelmie, et al., *Quantifying the Impact of Wind Turbine Wakes on Power Output at Offshore Wind Farms.* Journal of Atmospheric and Oceanic Technology, 2010. 27(8): p. 1302-1317.

[11] S.B. Roy, *Simulating impacts of wind farms on local hydrometeorology.* Journal of Wind Engineering and Industrial Aerodynamics, 2011. 99(4): p. 491-498.

[12] W. Zhang, C.D. Markfort, and F. Porté-Agel, *Experimental study of the impact of large-scale wind farms on land–atmosphere exchanges.* Environmental Research Letters, 2013. 8(1): p. 015002.

[13] G. Broström, *On the influence of large wind farms on the upper ocean circulation.* Journal of Marine Systems, 2008. 74(1–2): p. 585-591.

[14] M.J. Churchfield, Y. Li, and P.J. Moriarty, *A large-eddy simulation study of wake propagation and power production in an array of tidal-current turbines.* Philosophical Transactions of the Royal Society A: Mathematical, Physical and Engineering Sciences, 2013. 371(1985).

[15] S.W. Funke, P.E. Farrell, and M.D. Piggott, *Tidal turbine array optimisation using the adjoint approach.* Renewable Energy, 2014. 63(Supplement C): p. 658-673.
[16] S.R. Turnock, et al., *Modelling tidal current turbine wakes using a coupled RANS-BEMT approach as a tool for analysing power capture of arrays of turbines.* Ocean Engineering, 2011. 38(11): p. 1300-1307.
[17] R. Malki, et al., *Planning tidal stream turbine array layouts using a coupled blade element momentum – computational fluid dynamics model.* Renewable Energy, 2014. 63(Supplement C): p. 46-54.
[18] S.T. Fredriksson, et al., *Large eddy simulation of the tidal power plant deep green using the actuator line method.* IOP Conference Series: Materials Science and Engineering, 2017. 276(1): p. 012014.
[19] J.N. Sorensen and W.Z. Shen, *Numerical modeling of wind turbine wakes.* Journal of Fluids Engineering-Transactions of the Asme, 2002. 124(2): p. 393-399.